

Irreversible changes in doping efficiency and hydrogen bonding in the equilibrium state of *a*-Si:H

Xun-Ming Deng*

James Franck Institute and Department of Physics, The University of Chicago, Chicago, Illinois 60637

(Received 12 June 1990; revised manuscript received 26 October 1990)

We report unexpected irreversible changes in the conductivity (σ), dangling-bond density (DB), infrared-vibrational-absorption spectrum, and other properties of hydrogenated amorphous silicon (*a*-Si:H) by annealing samples above the glass transition temperature but below the deposition temperature. After annealing, both σ and the DB density decrease for P-doped samples, suggesting a decrease in donor-doping efficiency. For B-doped samples, both σ and the DB density increase after annealing, suggesting an increase in acceptor-doping efficiency. In the infrared-absorption spectrum, an increase at wave number 2085 cm^{-1} , together with a decrease at 1940 cm^{-1} with the same magnitude, and an increase at 620 cm^{-1} are observed after annealing. Possible explanations are discussed. No H effuses out of the sample during this irreversible annealing. Only a few percent of H rearranges its bonding. Our results show that *a*-Si:H is not in equilibrium after deposition but that it relaxes slowly to a more stable state above the equilibrium temperature.

I. INTRODUCTION

The discovery by Spear and LeComber¹ that hydrogenated amorphous silicon (*a*-Si:H) can be doped *n* type and *p* type by incorporating dopant atoms was one of the most important milestones in the field of amorphous semiconductors. This discovery was unexpected in view of the failure of doping vitreous chalcogenide semiconductors and the plausible explanation of this failure in terms of the natural tendency of atoms to seek a covalent coordination corresponding to their chemical valency and the freedom in noncrystalline semiconductors to do so. The success of doping *a*-Si:H was then attributed to the chance incorporation of some phosphorus or boron atoms in fourfold coordination. This could be expected to occur in amorphous materials such as amorphous silicon whose overconstrained structure was thought to be governed by the deposition process and not by equilibrium consideration of the kind used to explain the defect chemistry of chalcogenide glasses.^{2,3}

The first step toward understanding doping in *a*-Si:H was made by Street,⁴ who showed that the concentration of defects and dopants derive from an equilibrium reaction which at that time was believed to occur during sample preparation.

During the past few years our understanding of the equilibrium reactions between defects and dopants underwent a further remarkable development. A number of elegant experiments have shown that the concentrations of defects as well as of donors and acceptors are not fixed by the preparation conditions but that they change according to thermodynamic equilibrium reactions even at temperatures below that of deposition.⁵⁻¹²

These changes do not affect the atomic positions but the local bond configurations: atoms which deviate from their normal bonding coordination produce defect states in the gap or donors and acceptors, respectively. Different models were proposed to explain the creation and annealing of these excess defect states. Some suggest

that the structure can be changed by switching Si bonds, like the floating-bond model,¹² others suggest that the structure change is enabled by diffusion of hydrogen, like the H-glass model.¹³ In the H-glass model, the bond coordination changes are facilitated by the motion of hydrogen, the only atoms which change places in these defect and dopant reactions. Since the diffusion of hydrogen slows down exponentially with decreasing temperature, the defect and dopant equilibration process has a glasslike character with a glass transition or equilibration temperature T_E . Equilibration occurs very rapidly above T_E , within minutes near T_E , and exponentially slower below T_E .

A very interesting aspect of the glasslike thermal equilibrium kinetics is the interrelation between the atomic structure and the electronic properties. The Fermi level E_F is determined by the concentrations and gap energies of defects and dopants and in turn, the Fermi energy influences the magnitude of the formation energies of dopants and defects as well as of the hydrogen diffusion coefficient.¹⁴ As a result of this interrelation of hydrogen diffusion and E_F , the equilibrium temperature is about $T_E \sim 200^\circ\text{C}$ when E_F lies in the gap center and $T_E \sim 130^\circ\text{C}$ for *n*-type and $T_E \sim 100^\circ\text{C}$ for *p*-type material.¹³

The present research deals with the equilibrium state of doped and undoped *a*-Si:H above the equilibration temperature T_E . As we briefly reported earlier,¹⁵ we have observed substantial changes in the doping efficiency and the dangling-bond concentration as well as other properties as a result of long-term annealing above T_E but below the film deposition temperature. These irreversible relaxation processes have unexpectedly different effects on *n*-type and *p*-type samples.

II. EXPERIMENTAL DETAILS

Our samples were grown by plasma-enhanced chemical vapor deposition at 250°C on the grounded anode plate

at a rf power of 0.25 W/cm^2 . The flow rate of pure SiH_4 or SiH_4 containing the desired PH_3 and B_2H_6 dopant gases was 11 standard cubic centimeters per minute (sccm) at a pressure of 90 mTorr. These conditions yield high quality $a\text{-Si:H}$ films at a deposition rate of about 1 \AA/sec . The thickness of our samples range from 0.3 to $1 \text{ }\mu\text{m}$. Substrates of Corning 7059 glass, quartz, and crystalline Si are used for conductivity, photothermal deflection spectroscopy, and infrared absorption studies, respectively.

The samples were annealed at 220°C either in an inert gas atmosphere or in oil-free vacuum of a turbo molecular pump. The anneal temperature lies above the equilibration temperatures T_E of the samples and below the deposition temperature. At 220°C essentially no hydrogen is lost by evolution.

Conductivity measurements are performed in an oil-free vacuum chamber. Coplanar Mg electrodes separated by 0.2 cm are used for n -type samples and Ni-Cr for p -type samples. These electrodes are Ohmic up to 100 V. Samples were mounted with good thermal contact to a copper holder in oil-free vacuum. A water tube goes through this copper holder. When cold water flows through this tube, the samples are cooled down at a rate of about -30°C/sec . Slowly cooled states are obtained by cooling samples at a rate of 0.05°C/sec . Slow heating conductivity curves are measured when samples are warmed up with a rate of 0.1°C/sec .

Photothermal-deflection spectroscopy (PDS) is used to measure the subgap absorption, from which one calculates the defect density.¹⁶ In our PDS apparatus, the sample is mounted on a removable stainless-steel holder, which fits into a cell containing CCl_4 . The probing position is highly reproducible such that the PDS spectrum can be reproduced to within 5% as long as we do not remove the sample from the holder. The samples are annealed on their PDS holder in an inert gas atmosphere at 220°C . In this way, we obtain high reproducibility in the PDS spectra.

The infrared (ir) absorption spectra are measured with a Fourier transform infrared spectrometer (FTIR). In order to achieve high reproducibility the samples remain mounted on their holders all the time, even during annealing, so that we always measure the same area of the sample. For each spectrum, we take 700 FTIR scans and calculate the average by computer. This procedure reduces the noise level to less than 0.2% of the magnitude of the 2000-cm^{-1} absorption peak. The ir spectra are measured before and after annealing and stored by a computer which then subtracts the two spectra. This difference spectrum is the change in ir absorption due to annealing.

III. RESULTS

Figure 1 shows the conductivity curves of a lightly P-doped and a heavily B-doped sample, after the samples were annealed at 220°C for different times t_a . Both samples are $1\text{-}\mu\text{m}$ thick. The conductivity was measured while the samples are slowly heated following a slow cooling from elevated temperatures. Different doping levels are chosen here for n -type and p -type $a\text{-Si:H}$ in or-

der to compare samples with nearly the same conductivity.

The most striking result is that long time annealing irreversibly decreases the conductivity of n -type films while the conductivity of p -type films increases. A similar decrease in σ is observed in n -type $a\text{-Si:H}$ doped with arsenic as for phosphorus. The change in slope of the σ curves occurs at T_E . In order to measure T_E more accurately, we rapidly quenched the samples from high temperatures. We found that T_E increases with annealing. For the p -type sample T_E increased from 100 to 125°C after $t_a = 68 \text{ h}$. For the n -type sample T_E increased from 150 to 160°C . Figure 2 shows the logarithmic slope E_σ of the conductivity curves above 180°C as a function of annealing time t_a . The error is estimated by fitting straight lines in different ways between 180 and 220°C . Although the systematic error in the absolute value of E_σ may be large, the random error is suppressed by doing the experiment in a very systematic way. According to the equilibrium model the statistical shift of E_F is nearly compensated by the change in total carrier concentration so that E_σ is a measure of the distance of E_F from the transport level in the conduction and valence band, respectively.^{14,17} The decrease of E_σ in p -type and the increase of E_σ in n -type $a\text{-Si:H}$ with annealing time corresponds then to a net downward shift of E_F for both types

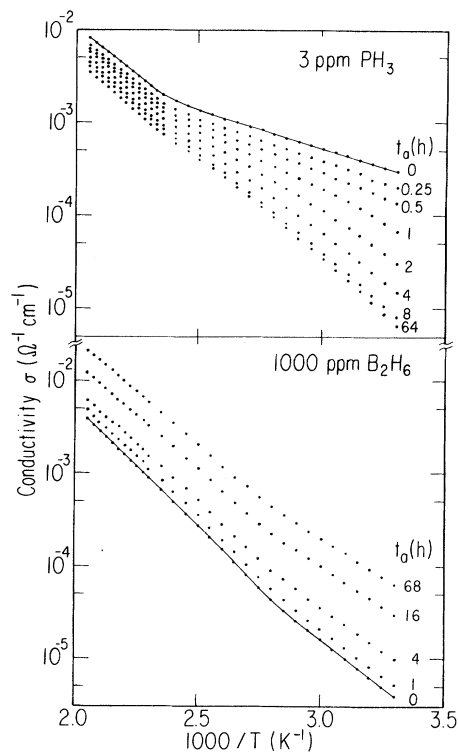


FIG. 1. Conductivity as a function of inverse temperature for 3-ppm-P-doped and 1000-ppm-B-doped $a\text{-Si:H}$, after different annealing times t_a (in h) at 220°C .

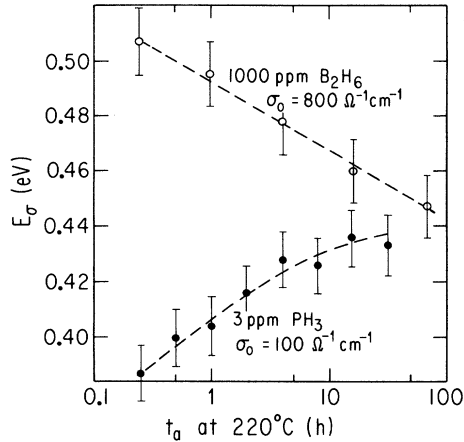


FIG. 2. Activation energy of the Arrhenius plot of conductivity in the section above T_E as a function of t_a for 3-ppm-P-doped and 1000-ppm-B-doped *a*-Si:H.

of samples. The rate of decrease with $\log t_a$ is nearly the same although the change appears to saturate in the *n*-type film after $t_a = 15$ h.

The conductivity prefactor σ_0 of the high-temperature sections of the σ curves does not change with annealing. We find $\sigma_0 = 100 \Omega^{-1} \text{cm}^{-1}$ for *n*-type film in agreement with the observations of others¹⁷ and a moderately higher value $\sigma_0 = 800 \Omega^{-1} \text{cm}^{-1}$ for the *p*-type film.

The substantial changes in the conductivities with annealing shown in Fig. 1 may result either from a change in the dangling-bond defect concentrations and/or a change in the doping efficiency.⁶ In order to distinguish these two effects we studied the change in defect concentration by measuring the subgap absorption by means of PDS. Figure 3 shows the effect of annealing on the absorption coefficients of the same two samples used for the conductivity studies. The points in the two dotted curves are original experimental data points. To get each point in the low absorption region, after the monochromator is moved to a new wavelength position, we wait for three minutes before measuring the signal for three minutes. Then the controlling computer takes the average over the three minutes to get the final data. The defect densities shown in the inset of Fig. 3 were calculated from the subgap absorption curves after subtracting the Urbach tail absorption. The errors are estimated from our experience. The larger error for the heavily doped *p*-type sample is due to the way to calculate defect density, since it is difficult to separate subgap absorption from the Urbach edge. The change in PDS subgap absorption is significant since the random error is less than 5% according to our experience. The high accuracy is achieved by leaving the sample on a PDS sample holder all the time, even during annealing. The sample can be put on and taken away from the system very reproducibly. In this way the random error is greatly suppressed. To make sure that we are not measuring surface defect in the PDS, we have etched the sample surface with 10%

hydrofluoric acid for 30 sec, a procedure to remove surface oxide. The obtained spectra before and after etching agree within 3%, indicating we are measuring bulk absorption.

If the decrease in σ of the *n*-type sample were caused by a change in dangling-bond defect concentration one would expect that more dangling bonds were converted from fourfold coordinated Si—Si bonds, hence expect to find a significant increase in subgap absorption. In contrast we find a small but noticeable decrease in the defect concentration of the *n*-type sample with annealing. The 20% decrease in PDS absorption is reasonably larger than the 5% error, and is reproducible in other samples. Conversely, the increase of the conductivity of the *p*-type sample might be thought of as resulting from a decrease in defect density. Again the opposite happens as shown in Fig. 3: the defect density increases with annealing in *p*-type samples. The dominant effect of annealing is therefore a change in the doping efficiency, it decreases in *n*-type and increases in *p*-type samples producing a net downward shift of the Fermi level.

As mentioned above, the equilibration temperature T_E increases with annealing in both *n*-type and *p*-type samples. Since T_E is related to hydrogen diffusion in the picture of the H-glass model, one suspects that annealing de-

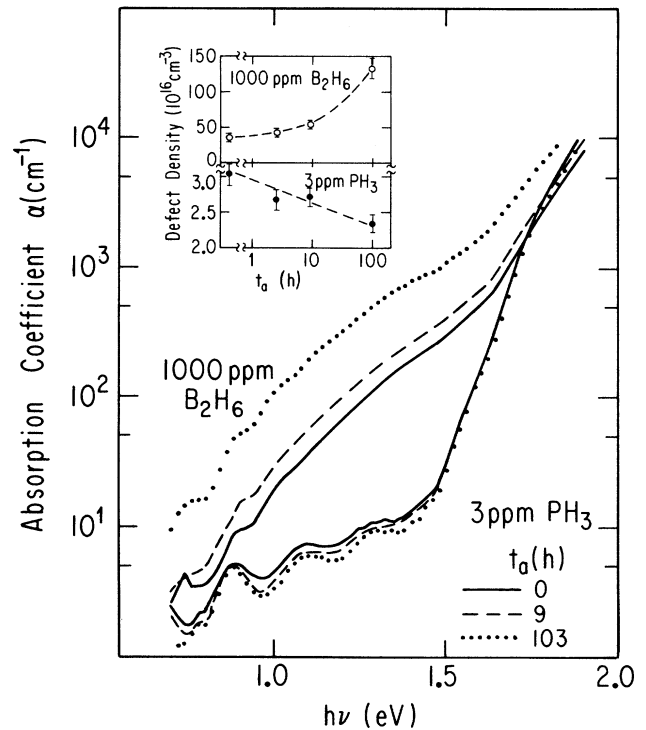


FIG. 3. Absorption coefficient measured with PDS as a function of photon energy for the 3-ppm-P-doped and 1000-ppm-B-doped *a*-Si:H after different annealing steps. The inset shows the defect density calculated from subgap absorption as a function of annealing time.

creases diffusion by allowing hydrogen to seek more stable bonding sites. In order to test this hypothesis we measured the effect of annealing on the infrared absorption bands that are associated with the Si—H stretching and bending modes.

Figure 4 shows the infrared absorption of a 10-ppm-P-doped (0.9- μm thick) and a 30-ppm-B-doped (1- μm thick) *a*-Si:H. The *y* axis is shifted for clarity. Figure 4(a) shows the spectra of these two samples before annealing. The peak centered at 2000 cm^{-1} is due to the silicon-hydrogen stretching mode and the one at 630 cm^{-1} is due to the silicon hydrogen wagging mode,¹⁸ from which we calculate the H content of these two samples¹⁹ and obtain 7.5 at. % for the 10-ppm-P-doped and 10.2 at. % for the 30-ppm-B-doped samples. By means of the computer we subtract the ir absorption spectrum of these two samples after annealing at 220 °C for 50 h with the one before annealing, to obtain the change in absorbance, Δ_{abs} , due to annealing, as shown in Fig. 4(b). One observes an increase in absorbance at 2085 cm^{-1} , a decrease at 1940 cm^{-1} with roughly the same magnitude, and an increase at 620 cm^{-1} . These changes also appear in samples with other doping levels, in compensated samples and in *pnpn* multilayers.

Because each spectrum is an average of 700 scans, the difference spectrum, Δ_{abs} , still has a high signal-to-noise ratio. Normally, on the average, the signal-to-noise ratio is about 40 after 50 h of annealing for the difference peaks around the 2000 cm^{-1} wave-number region. The

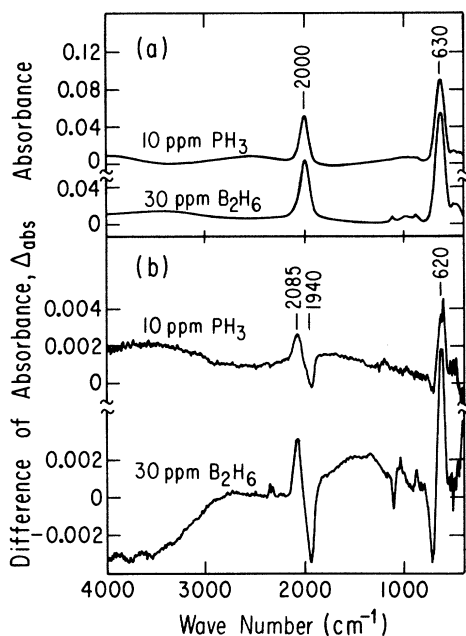


FIG. 4. (a) Infrared absorption spectrum of a 10-ppm-P-doped and a 30-ppm-B-doped *a*-Si:H. Vertical scale is shifted for clarity. (b) Difference of the absorption spectrum obtained by subtracting the spectrum before annealing from the one after 500 h of annealing at 220 °C.

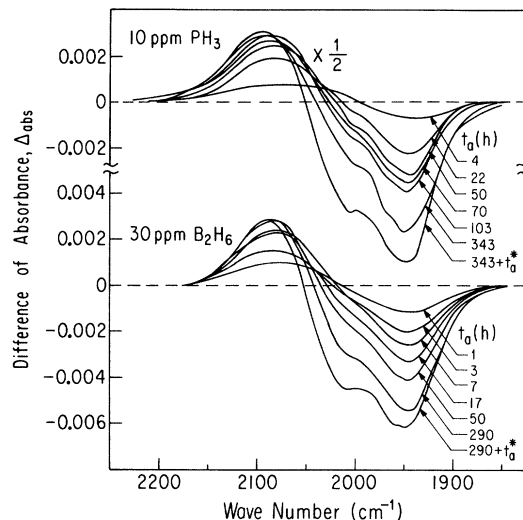


FIG. 5. Changes in absorbance of the 10-ppm-P-doped and 30-ppm-B-doped *a*-Si:H after being annealed at 220 °C for different times t_a . The symbol t_a^* denotes additional 30 h annealing at 250 °C.

large featureless change in the high-wave-number region is due to the instability of the FTIR spectrometer at different experimental times. It is irreproducible. The peaks around 2350 cm^{-1} are due to absorbance of CO_2 , which sometimes may not be completely eliminated from the light path in the spectrometer. The large features at the 1000–1200- cm^{-1} region cannot be suppressed by taking more scans. But these features are different for different samples and are very irreproducible.

Every time we measure the ir spectrum of samples after different annealing steps, we also measure the spectrum of a reference sample, which is not annealed at high temperatures. The reference sample also shows the features in the 1000–1200- cm^{-1} region but no feature near 2000 cm^{-1} . We conclude that the features in the 1000–1200- cm^{-1} region are either due to silicon oxide in the *c*-Si wafer or to an inhomogeneity in the *c*-Si wafer thickness because of the large absorbance of the relatively thick *c*-Si wafer compared to that of *a*-Si:H thin films. A tiny shift of the sample relative to the FTIR beam will result in a large change in the difference spectra in the region where *c*-Si absorbs strongly, if the *c*-Si wafer is inhomogeneous in either thickness or oxide content.

Figures 5(a) and 5(b) show an enlarged view of the 2000- cm^{-1} absorption difference for the two samples described in Fig. 4 after various annealing times t_a at 220 °C. The last annealing step (t_a^*) corresponds to additional 30 h at 250 °C after the previous annealing. The difference spectra can be deconvoluted into three Gaussians centered at 2085, 2000 and 1940 cm^{-1} , respectively. For $t_a < 50$ hours, the downward peak at 1940 cm^{-1} has nearly the same magnitude as the upward peak at 2085 cm^{-1} . Further annealing reduces the difference peak at

1940 cm^{-1} more, while keeping the 2085- cm^{-1} difference peak constant. A downward peak in the difference spectra at 2000 cm^{-1} becomes significant at long t_a , together with a decrease in absorbance at 630 cm^{-1} , which is negligible when $t_a < 50$ hours. This implies that no H has effused out of the material for $t_a < 50$ h while σ changes significantly; the change in ir spectra is mainly due to some rearrangement in H bonding.

To demonstrate the relation between the enhancement of ir absorption at the 2085- cm^{-1} peak with the one at 620 cm^{-1} , we plot the change in intensity:

$$\Delta I = \int \frac{\Delta \alpha d\bar{\nu}}{\bar{\nu}}, \quad (1)$$

with t_a for the 620- and 2085- cm^{-1} peaks in Fig. 6, where $\bar{\nu}$ is the wave number. ΔI_{620} and ΔI_{2085} show parallel behavior suggesting the same origin of the enhancement in absorption at 2085 and 620 cm^{-1} .

The fraction of infrared absorption that is transferred from 1940 to 2085 cm^{-1} relative to the total absorption band centered at 2000 cm^{-1} depends on the kind and concentration of doping. After annealing for 50 h at 220°C this fraction is largest (5.5%) for 30-ppm- B_2H_6 -doped samples; it is only 0.5–1% for undoped but increases again with increasing P doping from 2.5% at 10-ppm PH_3 to 4% at 100-ppm PH_3 . This trend mirrors that of hydrogen diffusion which increases as the Fermi level is moved away from the gap center but more so for p -type than for n -type samples.^{13,20} This relation is however not obeyed by compensated samples whose Fermi level lies at the gap center.^{13,20} Whereas the H diffusion in these is as small as in undoped samples, the fraction of hydrogen stretching modes transferred from low to higher wave numbers is 3% for a 100-ppm- PH_3 and 100-ppm- B_2H_6 compensated sample. The small transfer fraction of 0.5–1% has been observed in five different undoped samples.

The changes in the infrared absorption spectra appear to be irreversible. No recovery has been observed after keeping the two samples used for Fig. 5 at 150°C for 10 days or at room temperature for four months.

Whenever a -Si:H films are being annealed for extended periods of time one suspects that some hydrogen might have escaped the film, thereby changing the properties of the surface region. We conducted the following experi-

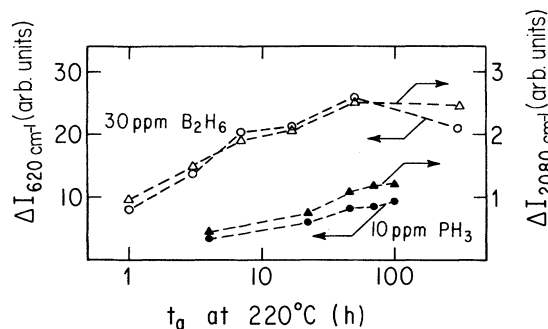


FIG. 6. The magnitude of the 620 cm^{-1} peak and the 2085- cm^{-1} peak as a function of annealing time at 220°C for the 10-ppm-P-doped and 30-ppm-B-doped a -Si:H.

ments in order to make sure that the observed irreversible changes in conductivity and ir absorption spectra are bulk effects.

We etched the surface of the P-doped samples after high-temperature annealing with saturated NaOH to remove 1000 Å of the a -Si:H from the surface. We find no recovery of the conductivity. In order to make sure that the increase in conductance of p -type samples after annealing is not due to a hole accumulation region near the surface,²¹ we exposed the sample to a flow of nitrogen containing 15% relative humidity. No decrease in conductance was observed which indicates that the buck conductance is dominating.²² Finally, we etched the samples used for the infrared absorption study. No change in the ir spectra was found after removing the oxide layer by a HF etch. Removal of a 1000-Å surface layer by saturated NaOH produced only a change in the magnitudes of the ir absorption features in proportion to the decrease in sample thickness. We therefore can eliminate any effects due to changes in the surface regions of the films.

IV. DISCUSSION

We have found that both defect and donor concentration decrease in n -type a -Si:H, and both defect and acceptor concentration increase in p -type a -Si:H after long-term annealing. These changes can be explained in a straightforward way with the following equations:



and



which were proposed by Stutzmann¹¹ and Street *et al.*⁶ Figure 7 is an example of a microscopic picture of Eq. (2). A fourfold-coordinated phosphorus $\text{P}_{(4)}^+$ and a doubly occupied dangling bond (D^-) coexist in the material, as shown in Fig. 7(a). With high-temperature annealing, the Si—P bond may be broken and the P atom may change to its threefold-coordinated form ($\text{P}_{(3)}^0$). The H then has a chance to diffuse to this newly created dangling-bond site. The dangling bond left over by the H can then recombine with the D^- to form a normal Si—Si bond as shown in Fig. 7(b). The microscope picture for Eq. (3) may be, as

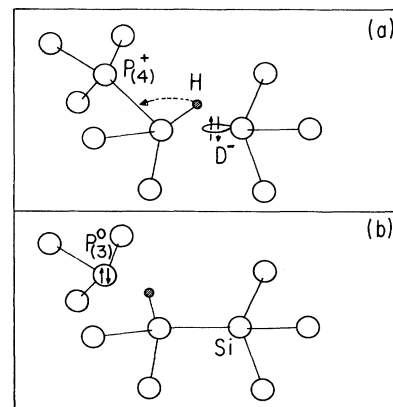


FIG. 7. Microscopic model for donor-defect reaction. See the discussion in the text.

an example, described by an opposite process of Fig. 7, from (b) to (a). In this case, $P_{(4)}^+$, $P_{(3)}^0$, and D^- should be replaced with $B_{(4)}^-$, $B_{(3)}^0$, and D^+ , respectively.

At the present time we do not have a clear explanation for the asymmetric changes in the dopant and defect concentration for the different types of doping. In the following, we will try to understand this asymmetry within the framework of different models.

In the free-energy-minimization model proposed by Street *et al.*,⁸ a single donor (acceptor) and defect level and a single band-tail-state level are first assumed. Then they use thermodynamic principles to calculate the total formation energy for the dopant defect pairs ($D^-P_{(4)}^+$ or $D^+B_{(4)}^-$) and the Fermi levels. They obtain for *n*-type samples

$$U(D^-P_{(4)}^+) = \frac{1}{2}[U_P + U_D - (E_P - E_{D^-})] \quad (4)$$

$$E_F = \frac{1}{2}(E_P + E_{D^-}) + \frac{1}{2}(U_D - U_P) - kT \left[1 + \frac{1}{2} \ln \left[\frac{N_0}{N_P} \right] \right], \quad (5)$$

and for *p*-type samples

$$U(D^+B_{(4)}^-) = \frac{1}{2}[U_B + U_D - (E_{D^+} - E_B)], \quad (6)$$

$$E_F = \frac{1}{2}(E_B + E_{D^+}) + \frac{1}{2}(U_B - U_D) + kT \left[1 + \frac{1}{2} \ln \left[\frac{N_0}{N_B} \right] \right], \quad (7)$$

where U_D , U_P , and U_B are the formation energies of neutral dangling-bond defects, neutral donors, and neutral acceptors, respectively, and E_P and E_B are the donor and acceptor gap energies, respectively. E_{D^-} and E_{D^+} are the gap energies of dangling bonds in *n*-type and *p*-type *a*-Si:H, respectively. N_0 , N_P , and N_B are the concentrations of potential defect sites and of dopants that can convert to donors and acceptors, respectively. The observed decrease of $D^-P_{(4)}^+$ pairs and the increase of $D^+B_{(4)}^-$ pairs with annealing may result from an increase in the formation energy $U(D^-P_{(4)}^+)$ and a decrease in $U(D^+B_{(4)}^-)$. As we mentioned earlier, for both types of samples, the Fermi levels move down in the gap with long-term annealing. In order to account for the changes in the right directions for these four parameters, we must assume according to Eqs. (4)–(7), an increase in U_P and a decrease in U_B or alternatively a decrease in both E_P and E_B . The present experiments would be the first indications for such relaxation-induced changes.

High-temperature annealing might relax the structure such that the number of weak Si—Si bonds is decreased resulting in a sharpening of the Urbach absorption edge. We have observed a small decrease of the Urbach-edge parameter E_0 with annealing at higher temperature. However this effect is not much larger than the experimental error. According to our present understanding of the defect reactions, a decrease in the energy E_{VB} of valence-band-tail states results in an increase in formation energy of defects. The consequence of this is a rise in E_F in *n*-type and a lowering of E_F in *p*-type samples. Such a symmetric effect contradicts our observations.

Winer and Street found²³ recently that dopants exist in

two bonding environments. In one the dopants can convert to donors or acceptors by changing to fourfold coordination. In the other the dopants are in a very stable threefold-coordination environment and thus remain inactive and do not convert. If the fraction of inactive dopants changes with annealing, this fraction must increase for phosphorus and decrease for boron dopants in order to account for our experimental results.

Jackson has proposed²⁴ that in *a*-Si:H doping and the Fermi level are determined by the equilibrium between H-passivated and unpassivated fourfold-coordinated dopants. In P-doped *a*-Si:H, fourfold-coordinated phosphorus can be passivated by a H atom at an adjacent tetrahedral site (T_d) of the adjacent Si and fourfold-coordinated B can be passivated by H at the bond-centered (BC) site of B and Si, as shown in Fig. 1 of the paper by Chang and Chadi²⁵ and Fig. 1 of Ref. 24. In this case, the annealing moves H away from the BC site in B-doped film and moves a H atom to the T_d site in P-doped film to account for the changes in doping efficiency.

Although it has been suggested that the dopant defect reactions are mediated through floating bonds, there is strong evidence that the kinetics is governed by the motion of hydrogen and that the relevant site energies depend on the local bonds to hydrogen. According to our experimental results, H in the material is moving from lower (1940 cm^{-1}) to higher (2085 cm^{-1}) vibrational energy sites (see Figs. 4 and 5) with long-term annealing. The concentrations of P—H and B—H bonds are unfortunately too low to be detected in our ir absorption experiments. It is however likely that the different chemical nature of P and B will affect the local bonding environment with hydrogen. This may lead to the asymmetric effect of annealing, an increase in doping efficiency in B-doped and a decrease in P-doped material.

At present we cannot identify the origin of the Si—H stretching modes that are centered at 1940 and 2085 cm^{-1} . A particular mode at 1940 cm^{-1} has not been observed before; the 2085 cm^{-1} is close to the value of 2100 cm^{-1} associated with the stretching vibration of dihydride. The two peaks of the difference spectra are separated by 145 cm^{-1} (see Fig. 4) and thus lie in the tail of the 2000-cm^{-1} monohydride absorption which has a full width at half maximum (FWHM) of 105 cm^{-1} .

In the following we discuss a possible origin for the 1940-cm^{-1} peak, which has never been observed before. It is found that in B-doped crystalline silicon containing H, there are Si—H—B chains. The existence of the acceptor (B) reduces the stretching vibrational frequency of the Si—H in the chain from wave number 2270 to 1880 cm^{-1} , as calculated theoretically^{25,26} and observed experimentally.²⁷ Chang and Chadi proposed²⁸ in crystalline Si a diatomic hydrogen complex H_2^* which consists of a H atom in the bond-centered site and another in an adjacent tetrahedral (T_d) site (see Fig. 1 of Ref. 28). The authors also suggested the diffusion mechanism for this complex. Recently, Jackson introduced²⁹ the H complex H_2^* to *a*-Si:H and explained many experimental results.

It is unlikely that the 1940-cm^{-1} vibrational mode is due to Si—H in the Si—H—B chain since we find that

6% of the total bonded H gets transferred from this wave number region. This is at least two orders of magnitude more than the concentration of B atoms in 30-ppm-B-doped *a*-Si:H. Since the amount of H transferred from 1940 cm^{-1} peak has the same order of magnitude as the H_2^* complex that Jackson proposed,²⁹ as shown in Fig. 1 of his paper, it is possible that the 1940- cm^{-1} peak is associated with the H in the H_2^* complex. The increase at the 2085- cm^{-1} peak indicates either more silicon dihydride or more of strongly bonded silicon monohydride in the material after annealing. Hence annealing changes the local bonding environment of Si—H bonds, probably creating more SiH_2 bonds.

It is interesting to note that for compensated *a*-Si:H the rate of hydrogen transfer with annealing from the 1940- to the 2085- cm^{-1} modes does not follow the normal trend of the hydrogen diffusion coefficient which is lowest when E_F lies near the gap center. The transfer rate of our undoped samples is very small indeed but for the compensated sample it is as high as those of *n*-type and *p*-type samples.

Recently, Asano and Stutzmann found³⁰ an irreversible change in the structure of B-doped *a*-Si:H after annealing at 220°C. They found nearly a factor of two decrease of the 2000- cm^{-1} wave-number peak in the ir spectrum of 2×10^{-2} -B-doped *a*-Si:H after 100 h of annealing at 220°C, and this decrease is stronger at the higher wave-number side of the peak. This observation is in contradiction to our finding that only a few percent of H has rearranged its bonding in the way that the lower-wave-number side of the 2000- cm^{-1} peak decreases while the higher-wave-number side increases. This disagreement is probably due to the difference in doping level, since H in such very heavily B-doped *a*-Si:H tends to diffuse out or change its bonding at a lower temperature.

V. SUMMARY AND CONCLUSIONS

We have observed irreversible changes in σ , the DB density, and the ir-vibrational-absorption spectrum of doped *a*-Si:H after annealing above the equilibrium temperature. A factor of 40 decrease in σ and 20% decrease in the DB density are found in 3-ppm-P-doped *a*-Si:H after 100 h annealing at 220°C, suggesting a decreasing in donor doping efficiency. The increase in both σ and the DB density in B-doped *a*-Si:H suggests an increase in acceptor-doping efficiency. Changes in doping efficiency have been observed earlier, as a result of light exposure at high temperature.^{31,32} But the light-induced change in doping efficiency is reversible and the annealing induced change is permanent. Therefore, different mechanisms are implied.

Besides the changes in doping efficiency, we find, in vibrational absorption spectrum, an increase at 2085 cm^{-1} , together with a decrease of the same magnitude at 1940 cm^{-1} , and with an increase at 620 cm^{-1} after annealing. No H has effused out of the sample or converted to infrared inactive H_2 , a few percent of H changes its bonding during annealing, which is probably a conversion of H from SiH to SiH_2 .

Freshly deposited *a*-Si:H is not in equilibrium; the material can relax to a more stable state through a very slow relaxation process.

ACKNOWLEDGMENTS

It is a great pleasure to thank my thesis advisor Professor Hellmut Fritzsche for his continued guidance and encouragement throughout this work. This work was supported by the National Science Foundation Grant No. DMR 8806197 and the University of Chicago Materials Research Laboratory funded by the National Science Foundation.

*Present address: Energy Conversion Devices, Inc., 1675 West Maple Road, Troy, Michigan 48084.

¹W. E. Spear and P. G. LeComber, *Philos. Mag.* **33**, 935 (1976).

²R. A. Street and N. F. Mott, *Phys. Rev. Lett.* **35**, 1293 (1975).

³M. Kastner, D. Adler, and H. Fritzsche, *Phys. Rev. Lett.* **37**, 1504 (1976).

⁴R. A. Street, *Phys. Rev. Lett.* **49**, 1187 (1982).

⁵R. A. Street and J. Kakalios, *Philos. Mag.* **B 54**, L21 (1986).

⁶R. A. Street, J. Kakalios, C. C. Tsai, and T. M. Hayes, *Phys. Rev. B* **35**, 1316 (1987).

⁷X.-M. Deng, *Bull. Am. Phys. Soc.* **33**, 227 (1988).

⁸R. A. Street, M. Hack, and W. B. Jackson, *Phys. Rev. B* **37**, 4209 (1988).

⁹Z. E. Smith and S. Wagner, *Phys. Rev. B* **32**, 5510 (1985).

¹⁰Y. Bar-Yam, D. Adler, and J. D. Joannopolus, *Phys. Rev. Lett.* **57**, 467 (1986).

¹¹M. Stutzmann, *Phys. Rev. B* **35**, 9375 (1987).

¹²S. T. Pantelides, *Phys. Rev. Lett.* **57**, 2979 (1986); **58**, 1344 (1987).

¹³J. Kakalios and W. B. Jackson, in *Amorphous Silicon and Related Materials*, edited by H. Fritzsche (World Scientific, Singapore, 1989), p. 207.

¹⁴R. A. Street, *Phys. Rev. B* **43**, 2454 (1991).

¹⁵H. Fritzsche and X.-M. Deng, *Bull. Am. Phys. Soc.* **35**, 349 (1990).

¹⁶W. B. Jackson and N. M. Amer, *Phys. Rev. B* **25**, 5559 (1982).

¹⁷J. Kakalios and R. A. Street, *Phys. Rev. B* **34**, 6014 (1986).

¹⁸G. Lucovsky, *Solar Cells* **2**, 431 (1980).

¹⁹H. Shanks, C. J. Fang, L. Ley, M. Cardona, F. J. Demond, and S. Kalbitzer, *Phys. Status Solidi B* **100**, 43 (1980).

²⁰R. A. Street, C. C. Tsai, J. Kakalios, and W. B. Jackson, *Philos. Mag.* **B 56**, 305 (1987).

²¹B. Aker and H. Fritzsche, *J. Appl. Phys.* **54**, 6628 (1983).

²²M. Tanielian, *Philos. Mag.* **B 45**, 435 (1982).

²³K. Winer and R. A. Street, *Phys. Rev. Lett.* **63**, 880 (1989).

²⁴W. B. Jackson, *Phys. Rev. B* **41**, 12 322 (1990).

²⁵K. J. Chang and D. J. Chadi, *Phys. Rev. Lett.* **60**, 1422 (1988).

²⁶G. G. DeLeo and W. B. Fowler, *Phys. Rev. B* **31**, 6861 (1985).

²⁷M. Stavola, S. J. Pearton, J. Lopata, and W. C. Dautremout-Smith, *Appl. Phys. Lett.* **50**, 1086 (1987).

²⁸K. J. Chang and D. J. Chadi, *Phys. Rev. Lett.* **62**, 937 (1989).

²⁹W. B. Jackson, *Phys. Rev. B* **41**, 10 257 (1990).

³⁰A. Asano and M. Stutzmann, *Phys. Rev. B* **42**, 5388 (1990).

³¹X.-M. Deng and H. Fritzsche, *Phys. Rev. B* **36**, 9378 (1987).

³²J.-H. Yoon, M.-S. Kim, and C. Lee, *J. Non-Cryst. Solids* **114**, 636 (1989).